



HAL
open science

Unraveling the confusion over the iron oxidation state in MORB glasses

Antoine Bézos, Christèle Guivel, Carole La, Thibault Fougeroux, Eric Humler

► To cite this version:

Antoine Bézos, Christèle Guivel, Carole La, Thibault Fougeroux, Eric Humler. Unraveling the confusion over the iron oxidation state in MORB glasses. *Geochimica et Cosmochimica Acta*, 2021, 293, pp.28 - 39. 10.1016/j.gca.2020.10.004 . hal-03494044

HAL Id: hal-03494044

<https://hal.science/hal-03494044v1>

Submitted on 21 Nov 2022

HAL is a multi-disciplinary open access archive for the deposit and dissemination of scientific research documents, whether they are published or not. The documents may come from teaching and research institutions in France or abroad, or from public or private research centers.

L'archive ouverte pluridisciplinaire **HAL**, est destinée au dépôt et à la diffusion de documents scientifiques de niveau recherche, publiés ou non, émanant des établissements d'enseignement et de recherche français ou étrangers, des laboratoires publics ou privés.



Distributed under a Creative Commons Attribution - NonCommercial 4.0 International License

1 Unraveling the confusion over the iron oxidation state in
2 MORB glasses

3 Antoine Bézos^{a,*}, Christèle Guivel^a, Carole La^a, Thibault Fougeroux^a, Eric
4 Humler^a

5 ^a*Laboratoire de Planétologie et Géodynamique, LPG Nantes, CNRS UMR 6112,*
6 *Université de Nantes, 4 rue de la Houssinière, 44322, Nantes*

7 **Abstract**

The oxidation state of iron in mantle-derived melts is commonly used to determine the oxygen fugacity (fO_2) of magmas and their related sources. The accurate and precise determination of the iron oxidation state ratio of Mid-Oceanic Ridge Basalt (MORB) glasses has been a matter of controversy for the last three decades. None of the wet chemical methods used in the literature to measure this ratio converge toward a consensus value. The same difficulties have been observed for the most recent data obtained by XANES spectroscopy, which allows the measurement of the iron oxidation state ratio at high spatial resolution. This study unravels the origin of the analytical biases observed between the colorimetric and direct titration wet chemistries used in the studies of Christie et al. (1986) and Bézos and Humler (2005), respectively. We demonstrate that colorimetric measurements overestimate the ferrous iron contents of sulfide-bearing samples whereas the direct titration method does not suffer from such sulfide interference. Because MORB glasses contain significant amount of sulfur in the +2 valence state, we re-assessed the average MORB FeO/FeO_{total} ratio by using the bulk FeO_{total} and FeO data from this study and from Bézos and Humler (2005),

Preprint submitted to Elsevier
Corresponding author: antoine.bezos@univ-nantes.fr

September 18, 2020

respectively. We calculated for 49 MORB glasses an average $\text{FeO}/\text{FeO}_{\text{total}}$ of 0.90 ± 0.02 . This result agrees with colorimetric measurements corrected for sulfide interference and with the results of Bézou and Humler (2005), if corrected for the presence of plagioclase in the sample powders. The average MORB $\text{FeO}/\text{FeO}_{\text{total}}$ that we determined in this study agrees also within uncertainty with the most recent XANES spectroscopic data of Berry et al. (2018) (0.90 ± 0.02).

8 *Keywords:* MORB, iron, oxidation state, wet chemistry, XANES
9 spectroscopy

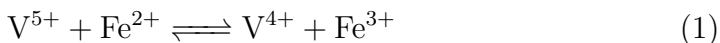
10 **1. Introduction**

11 The oxygen fugacity ($f\text{O}_2$) is a fundamental parameter that plays a role
12 in producing the calc-alkaline and tholeiitic differentiation trends (Gill, 1981;
13 Grocke et al., 2016; Chin et al., 2018), in determining the speciation of the
14 magmatic gases released into the atmosphere (Holland, 2002; Brounce et al.,
15 2017), and in influencing the valence state and partitioning behaviors of re-
16 dox sensitive elements in magmas. Iron is the only major element for which
17 two valence states co-exist in terrestrial mafic magmas. Therefore, special
18 attention has been paid to develop precise and accurate analytical methods
19 to measure the $\text{Fe}^{3+}/\Sigma\text{Fe}$ ratio (Mysen et al., 1985; Fialin et al., 2004; Bézou
20 and Humler, 2005; Cottrell and Kelley, 2011; Shorttle et al., 2015; Zhang
21 et al., 2018; Berry et al., 2018; Le Losq et al., 2019; Gaborieau et al., 2020)
22 and to relate this ratio to $f\text{O}_2$ (Kress and Carmichael, 1991; O'Neill et al.,
23 2018). The $\text{Fe}^{3+}/\Sigma\text{Fe}$ ratio of MORB magmas has been regularly debated in
24 the literature during the last three decades (Carmichael and Ghiorso, 1986;

25 Christie et al., 1986; Bézos and Humler, 2005; Cottrell and Kelley, 2011;
26 Zhang et al., 2018; Berry et al., 2018). There is yet no real consensus on
27 the absolute value of this ratio. This is mainly due to the analytical difficul-
28 ties encountered to measure the $\text{Fe}^{3+}/\Sigma\text{Fe}$ ratio using either the Mössbauer
29 spectroscopy method (Mysen et al., 1985; Rossano et al., 1999; Cottrell and
30 Kelley, 2011; Zhang et al., 2018; Berry et al., 2018), which is used to cali-
31 brate the results of XANES spectroscopy, or wet chemical methods (Christie
32 et al., 1986; Bézos and Humler, 2005). Important variations are observed in
33 the iron redox state ratio of basic magmas from different tectonic settings
34 (Kelley and Cottrell, 2012; Brounce et al., 2015; Gaborieau et al., 2020), and
35 even within a given setting (Sinton, 2003; Brounce et al., 2017; Hartley et al.,
36 2017; Novella et al., 2020). The lack of analytical consistency in the $\text{Fe}^{3+}/\Sigma\text{Fe}$
37 ratio measurements severely obscures our global view and understanding of
38 present and past earth magma's $f\text{O}_2$.

39 The main analytical challenge of wet chemistries relies on the preservation
40 of the iron redox state during sample digestion (Yokoyama and Nakamura,
41 2002). On this point, the studies of Christie et al. (1986) and Bézos and
42 Humler (2005) have followed different strategies using the colorimetric and
43 direct titration methods, respectively. In the former method, the sample is
44 dissolved at room temperature for several days, in the presence of a strong
45 oxidising agent: the pentavalent vanadium. The ferrous iron released from
46 the sample matrix is thus immediately oxidized in ferric iron by V^{5+} (eq.
47 1), which preserves the sample from uncontrolled oxidation by air (Wilson,

48 1960).



49 This problem of Fe^{3+} oxidation by atmospheric O_2 has been investigated
50 by Bézoz and Humler (2005) in the context of a quite different sample dis-
51 solution protocol, which involved hot boiling acids for three minutes. The
52 authors compare FeO measurements of vanadium-free dissolutions performed
53 under inert (Ar) and ambient atmospheres. The results of these experiments
54 show no evidence of accidental Fe^{2+} oxidation by air.

55 On the other hand, the issue of the reduction of ferric to ferrous iron
56 by sample sulfides during sample digestion has often been invoked (Wilson,
57 1960; Saikkonen and Rautiainen, 1993; Sossi and O’Neill, 2011; Berry et al.,
58 2018), but never demonstrated for the case of oceanic basaltic glasses anal-
59 yses. Nonetheless, the accurate measuring of the iron redox state ratio in
60 MORB glasses requires a thoughtful evaluation of the potential interference
61 of sulfides during sample dissolution. For this purpose, we used the colori-
62 metric method — optimised to measure both FeO and FeO_{total} in the same
63 aliquot of solution — and determined the FeO/FeO_{total} ratios of 6 reference
64 materials and 49 MORB glassy samples. We quantified the interference of
65 S^{2-} on the colorimetric and direct titration methods and proposed a re-
66 evaluation of the average FeO/FeO_{total} of MORB glasses (0.90 ± 0.02). We
67 compared this results to the most recent XANES spectroscopic data cali-
68 brated by Mössbauer spectroscopy (Cottrell and Kelley, 2011; Zhang et al.,
69 2018; Berry et al., 2018).

70 **2. Reference materials and MORB samples**

71 We analysed 6 natural reference powders of mafic rocks, BE-N, BR,
72 BHVO-1, BCR-1, W-2 and JB-2 (see Table A1 and A2 in appendix A).
73 They display recommended total iron contents, FeO/FeO_{total} ratios, and sul-
74 fur contents ranging from 9.5 to 13 wt. %, 0.56 to 0.87, and 20 to 400 μ g/g,
75 respectively (Govindaraju, 1994; Jochum et al., 2016).

76 From the 49 Mid-Oceanic Ridge Basaltic (MORB) glassy samples selected
77 from global sources, forty-six correspond to the same sample powders anal-
78 ysed by Bézou and Humler (2005) and/or Christie et al. (1986). Three new
79 MORB glasses are specific to our study. They come from the South West In-
80 dian (ED-DR1-1-1), South East Indian (MD57-D2-3) and the Mid-Atlantic
81 (MAPCO CH98-DR07) ridges (Bézou, 2003). All powders correspond to
82 chips of glass that have been carefully hand-picked under a binocular micro-
83 scope to discard all visible signs of alteration or micro-phenocrysts and were
84 gently hand-ground in agate mortar (Christie et al., 1986; Bézou and Humler,
85 2005).

86 **3. Colorimetric FeO/FeO_{total} analyses**

87 The colorimetric method derives from the experimental protocols devel-
88 oped by Wilson (1960) and Schuessler et al. (2008). When used conjointly,
89 these two protocols allow the determination of the FeO/FeO_{total} ratio in the
90 same sample aliquot. The basic principle of FeO colorimetric measurements
91 relies on the introduction of an oxidising agent (V^{5+}) before sample digestion
92 to prevent undesired and accidental oxidation of Fe^{2+} (Wilson, 1960). As the
93 digestion proceeds and breaks down the silicate network, the ferrous iron re-

94 leased into the low pH acid solution is immediately oxidised into ferric iron
95 by pentavalent vanadium (eq. 1). The excess of V^{5+} during sample digestion
96 ensures the quantitative oxidation of all Fe^{2+} into Fe^{3+} . Once the digestion
97 is completed, the addition of an acetate buffer increases the pH of the so-
98 lution up to 5. The reaction 1 is therefore reversed and proceeds now from
99 right to left. The initial ferrous iron thereby regenerated can be analyzed by
100 colorimetry (Wilson, 1960). The total iron content is then measured in its
101 ferrous form by adding a strong reducing agent to convert all the remaining
102 Fe^{3+} into Fe^{2+} (Schuessler et al., 2008).

103 3.1. FeO/FeO_{total} analytical protocol

104 About 3-7 mg of sample powders were weighed with a precision of 10^{-3} mg
105 in 7 mL crystal polypropylene beakers and digested for three days at room
106 temperature in a mixture of 1 mL HF (40%) and 1mL of 1.41×10^{-2} mol.L⁻¹
107 ammonium vanadate solution to guarantee V^{5+} excess. After complete di-
108 gestion, 5 mL of beryllium sulfate solution (2.82 mol.L⁻¹) were added to the
109 beakers to neutralise the excess of HF and to break down all insoluble fluo-
110 rides. The prepared solutions were then transferred into 100 mL borosilicate
111 glass volumetric flasks containing 10 mL ammonium acetate buffer solution
112 (6.48 mol.L⁻¹) and 5 mL of a 2:2'-dipyridyl colorimetric reagent solution (6.9
113 $\times 10^{-3}$ mol.L⁻¹). All the flasks were then filled up to 100 mL with ultra-pure
114 water. All samples and procedural blanks were stirred for 20 minutes before
115 analysis to ensure full homogeneity of the solutions. The FeO_{total} analyti-
116 cal solutions were prepared by adding 100 mg of the strong reducing agent
117 hydroxylamine hydrochloride to 15 mL of the FeO solutions. We prepared
118 ferrous stock solution at 3.7×10^{-2} mol.L⁻¹ by dissolving 14.5 g of ammonium

119 ferrous sulfate hexahydrate in 1L 2.9 % (m/m) H₂SO₄. This stock solution
120 was then diluted to 0.0014 mol.L⁻¹ and used to prepare the FeO and FeO_{total}
121 external standard calibration solution at 2, 4, 6, 8, and 9.5 mg.L⁻¹ Fe²⁺.

122 3.2. Spectroscopic measurements

123 All colorimetric measurements reported in this study were acquired with
124 the UV/VIS spectrophotometer CARY UV 500 (Varian) of the Laboratoire
125 de Planétologie et Géodynamique (LPG, Université de Nantes, France). The
126 optical density measurements were done at 525 nm where the ferrous- 2:2-
127 dipyridil complex absorption is maximum (Wilson, 1960). All peak heights
128 were determined relative to the baseline measured at 700 nm. The FeO/FeO_{total}
129 ratios were determined by dividing the absorbance signals corrected for the
130 baseline measured at 700 nm and for the procedural blanks. The typical
131 regression parameters obtained for our external FeO and FeO_{total} standard
132 calibrations display $r^2 = 0.9999$ and intercepts that range between $-0.01 \pm$
133 $0.02 (1\sigma)$.

134 4. Analytical experiments in presence of sulfide

135 The presence of reduced species such as sulfide (S²⁻) in natural samples
136 has often been invoked as a potential source of interferences during FeO wet
137 chemistries (Saikkonen and Rautiainen, 1993; Cottrell and Kelley, 2011; Sossi
138 and O'Neill, 2011; Berry et al., 2018). Below, we present the experimental
139 protocols that we have designed to characterise and quantify the potential
140 sulfide interference on colorimetric and direct titration FeO measurements.

141 *4.1. Cold sample digestion in presence of vanadium (colorimetric method)*

142 We used simple S^{2-} , Fe^{3+} and V^{5+} reagent solutions to quantify the redox
143 reactions that occur between these species during the three-day low temper-
144 ature sample digestion.

145 In a first experiment, a synthetic solution of S^{2-} at 4.16×10^{-2} mol.L⁻¹
146 was prepared by dissolving sodium sulfide hydrated salts ($Na_2S \cdot 9H_2O$) in
147 pure H_2O . We then poured 0.1 g of $NH_4 \cdot VO_3$ salt (V^{5+}) into 5 mL of the S^{2-}
148 solution and let the mixture rest at room temperature for between one hour
149 and 72 hours. The titration of the V^{5+} left after the redox reaction with S^{2-}
150 was done using a solution of Fe^{2+} (3.69×10^{-2} mol.L⁻¹) with 10 mL of pure
151 H_2O and 10 mL of the coloured indicator barium diphenylamine sulfonate
152 prepared following Crabtree and Lange (2012). The same protocol was then
153 duplicated but without the addition of S^{2-} . The difference between the two
154 titrations quantifies the number of S^{2-} moles that has reacted with V^{5+} .

155 In a second experiment, we tested the potential reaction between the S^{2-}
156 and Fe^{3+} species. We poured 5 mL of the S^{2-} solution (4.16×10^{-2} mol.L⁻¹)
157 into 20 mL of Fe^{3+} solution at 4×10^{-2} mol L⁻¹ and let it rest between 1 and
158 72 hours at room temperature. The titration of the Fe^{2+} was done using a
159 solution of Cr^{6+} solution at 6.2×10^{-3} mol.L⁻¹, 5 mL of barium diphenylamine
160 sulfonate as a coloured indicator and a few drops of concentrated HCl to lower
161 the pH of the solution for titration.

162 Finally, the third experiment follows the conceptual approach of the stan-
163 dard addition method. We selected two MORB glassy samples that display
164 natural sulfur contents of 1400 $\mu g/g$ for the JDF-D2 and 1128 $\mu g/g$ for GN02-
165 02 (Bézos, 2003). We dissolved 3 aliquots of each sample in the exact same

166 conditions as those described in section 3.1 and added for two of them varying
167 amounts of S^{2-} solution — one aliquot remained therefore free of S^{2-} addition.
168 The FeO/FeO_{total} ratio, FeO and FeO_{total} contents were then measured by
169 colorimetry.

170 *4.2. Hot sample digestion in absence of vanadium (direct titration method)*

171 Following the analytical protocol of Bézoz and Humler (2005), we proceed
172 to several dissolutions of the BR basaltic reference material with, and without
173 the addition of a S^{2-} prior to sample digestion. The sample powder batches
174 (≈ 0.5 g) were then dissolved during three minutes in a mixture of boiling
175 sulfuric and hydrofluoric acids. The released ferrous iron was immediately
176 titrated against a potassium dichromate solution in a mixture of H_2SO_4 and
177 H_3PO_4 , using barium diphenylamine sulphonate as the redox indicator (for
178 more details see Bézoz and Humler, 2005).

179 **5. Results**

180 Historically, we have become used to report the iron redox state in the
181 form of the $Fe^{3+}/\Sigma Fe$ ratio, which corresponds to the ratio of the quantity of
182 Fe_2O_3 normalized to the total iron expressed as ferric iron. Because only few
183 wet chemical methods are available to determine the ferric iron in geological
184 samples (Roex and Watkins, 1995; Tarafder and Thakur, 2013), this latter
185 oxide is usually recalculated by difference between FeO_{total} — the total iron
186 expressed as ferrous iron — and FeO measurements. However, for the sake
187 of analytical consistency and coherent error propagation calculations, we
188 consider that it is more relevant to present our results in the form of the

189 FeO/FeO_{total} ratio. Both ratios are related by the relationship $\text{Fe}^{3+}/\Sigma\text{Fe} =$
190 $1 - \text{FeO}/\text{FeO}_{\text{total}}$.

191 *5.1. Colorimetric measurements on geological reference materials*

192 Comparisons of our FeO_{total}, FeO, and FeO/FeO_{total} measurements with
193 recommended (Govindaraju, 1994; Jochum et al., 2016) or previously pub-
194 lished (Bézos and Humler, 2005) values are presented in Fig.1 (see also Table
195 A.1 in supplementary materials). Although, the FeO_{total} data are offset on
196 average by 0.20% FeO_{total} above the 1:1 line in Fig. 1-A, our results agree
197 within 2 sigma error with the recommended values of Jochum et al. (2016),
198 except for BHVO-1. Our FeO and FeO/FeO_{total} results match all reference
199 values, except for the FeO/FeO_{total} ratio of BHVO-1 (Fig. 1-B and -C). The
200 reproducibility of our measurements varied between 0.6 and 2.2% (1σ rela-
201 tive) for FeO, 0.5 and 1.8% (1σ relative) for FeO_{total}, and from 0.5 to 1.2%
202 for the FeO/FeO_{total} ratio (Table A.1).

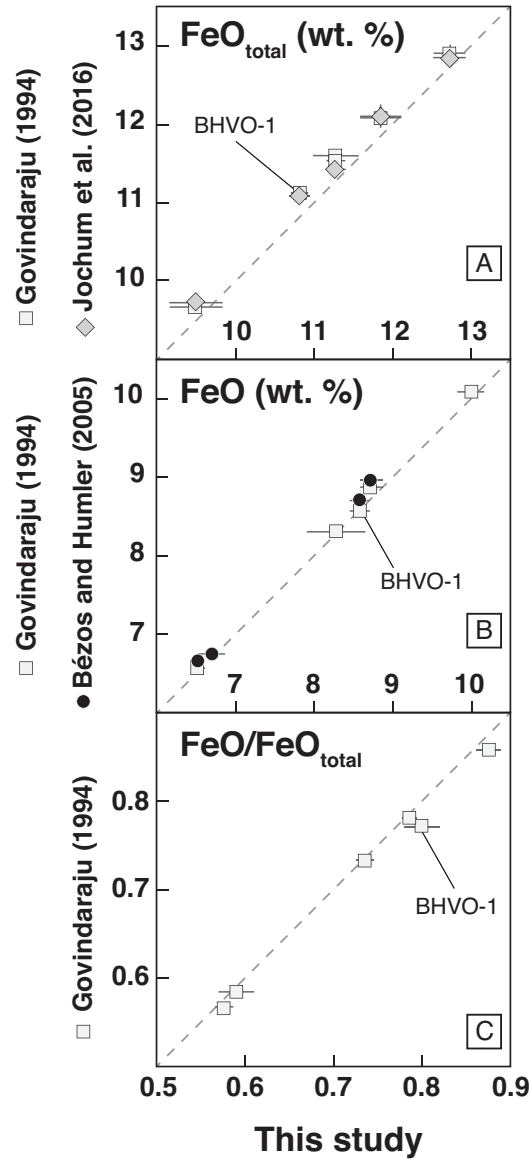


Figure 1: Comparison of $\text{FeO}_{\text{total}}$ (A), FeO (B), and $\text{FeO}/\text{FeO}_{\text{total}}$ (C) results from this study with recommended values from Govindaraju (1994) (white squares), preferred values from Jochum et al. (2016) (grey diamonds), and with Bézou and Humler (2005) (black dots) for 6 reference materials of mafic compositions. Dashed line: 1:1 line, error bars are 2σ errors.

205 *5.2. Colorimetric measurements on MORB glassy samples*

206 To begin with, it is important to remind briefly the discrepancies of the
207 analytical protocols used by Bézou and Humler (2005), Christie et al. (1986)
208 and this study. The present study and that of Christie et al. (1986) display
209 the closest match in their analytical methodologies. Indeed, both studies
210 determined the bulk FeO and $\text{FeO}_{\text{total}}$ contents for the same powder aliquots
211 and both studies used the same vanadium-based FeO colorimetric method,
212 which involves the cold dissolution of less than 10 mg of sample during three
213 days (Wilson, 1960). The only notable difference would be that Christie et al.
214 (1986) analyzed the bulk $\text{FeO}_{\text{total}}$ contents using a Direct Current Plasma
215 (DCP) spectrometer instrument whereas we used the colorimetric method
216 adapted from Schuessler et al. (2008). The differences between Bézou and
217 Humler (2005) and this study are, however, more fundamental. Bézou and
218 Humler (2005) analyzed the FeO contents by direct titration using a Cr^{6+}
219 solution (Grillot et al., 1964), which does not require pentavalent vanadium.
220 Moreover, the sample digestion in Bézou and Humler (2005) which involved
221 500 mg of material, was performed during 3 minutes above the boiling point
222 of an acid mixture composed of 7 mL of H_2SO_4 (9 mol.L⁻¹) and 3 mL HF (22

223 mol.L⁻¹). Finally, Bézou and Humler (2005) analyzed the FeO_{total} contents
224 using the in-situ electron microprobe technique. Some discrepancies between
225 the bulk colorimetric or DCP methods (Christie et al., 1986, and this study)
226 and the in-situ FeO_{total} electron microprobe data (Bézou and Humler, 2005)
227 may occur. Indeed, we cannot guarantee that the sample powders were
228 totally devoid of micro-crystals of plagioclase or olivine. The presence of the
229 former mineral has the effect to lower the measured iron content whereas the
230 latter increases it.

231 The 13 replicate analyses of the GN02-02 MORB powder over a period of 3
232 years yielded a reproducibility (relative 1 σ error) of 0.74% for FeO, 1.12% for
233 FeO_{total}, and 1.17% for the FeO/FeO_{total} ratio (Table A.2 in supplementary
234 materials). All other MORB results are reported in Table A.3 and presented
235 in Fig. 2. In Fig.2-A our FeO_{total} colorimetric results on MORB glasses dis-
236 play systematically lower values (\approx -0.28 wt.% on average) when compared
237 to microprobe data (Bézou and Humler, 2005, black dots). Although this
238 offset is comparable to that observed in Fig. 1-A, the good match between
239 our FeO_{total} results and that of bulk DCP analysis from Christie et al. (1986)
240 (white dots) strongly support that this offset is more likely related to the
241 use of bulk and in-situ analytical methods. As proposed by Bézou and Hum-
242 ler (2005) the presence of \approx 1.5% plagioclase micro-crystals — an iron-free
243 phase — in sample powders may account for the offset observed in Fig. 1-A.
244 In Fig. 2-B, our FeO data display on average higher contents (+0.21 wt.%
245 on average) when compared to the direct titration data of Bézou and Humler
246 (2005). Because both data sets were produced from the exact same batches
247 of powders with bulk analytical methods, such difference cannot be explained

248 by the presence of plagioclase micro-crystals in the powders. The FeO colorimetric data from our study match with that of Christie et al. (1986). Finally, 249 we report an average $\text{FeO}/\text{FeO}_{\text{total}}$ ratio of 0.92 ± 0.01 for our MORB sample set, which is in good agreement with the study of Christie et al. (1986). 250 251

252 The MORB data presented in Fig. 2 thus reveal a methodological bias between bulk and in-situ $\text{FeO}_{\text{total}}$ analyses and an analytical bias between 253 vanadium-based (Christie et al., 1986, this study) and direct titration FeO data (Bézos and Humler, 2005). 254 255

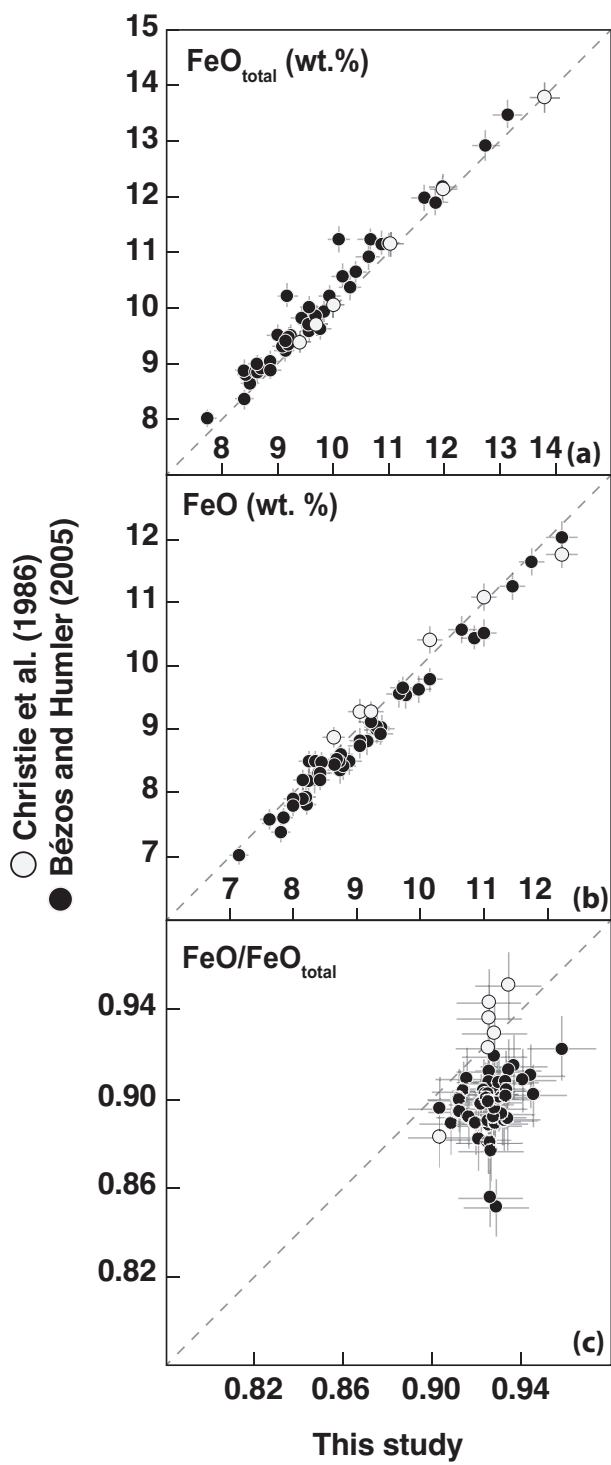


Figure 2: Comparison of $\text{FeO}_{\text{total}}$ (A), FeO (B) and $\text{FeO}/\text{FeO}_{\text{total}}$ (C) measurements from this study with results from Christie et al. (1986) (white dots) and Bézoz and Humler (2005) (black dots). The analyses were made on the same batches of powders. Error bars corresponds to a 95% confidence level. Dashed line: 1:1 line.

258 5.3. Sulfide interferences on FeO measurements

259 5.3.1. Colorimetric method

260 In a first experiment, we investigated the redox reaction that might oc-
 261 cur between pentavalent vanadium and sulfide during sample digestion. We
 262 prepared a solution with known amounts of S^{2-} and V^{5+} that we set aside at
 263 room temperature for one to 72 hours. We then titrated the amount of V^{5+}
 264 left in the final solution with a Fe^{2+} solution (all the results are in Table B.1
 265 in supplementary materials). From this data, we calculated the amount of
 266 V^{4+} formed during the redox reaction with S^{2-} and determined a $n_{\text{V}^{4+}}/n_{\text{S}^{2-}}$ -
 267 molar ratio of 1.9 ± 0.1 for this reaction. In the context of ferrous colorimet-
 268 ric measurements, the presence of V^{4+} implies that when eq. 1 is reversed,
 269 the number of mole of V^{4+} is not equal to $n_{\text{Fe}^{2+}}$ but to $n_{\text{Fe}^{2+}} + 1.9 \pm 0.1 \times$
 270 $n_{\text{S}^{2-}}$.

271 In a second experiment, we tested more specifically the potential inter-
 272 ference of S^{2-} on Fe^{3+} during sample digestion. We prepared 25 mL of a
 273 solution with known quantities of sulfide and ferric iron and left the solution
 274 at room temperature for one to 72 hours. During this experiment, we no-
 275 ticed the formation of black solid particles. After one night, the black solid
 276 turned into white solid. Raman spectroscopy of these particles revealed that

277 the black solids corresponds to FeS mackinawite and white solids to sulfur
278 α -S₈ (Bourdoiseau et al., 2008). Because of the presence of particles, the
279 solution was centrifuged and the Fe²⁺ formed was determined in a 20 mL
280 aliquot using a direct Cr⁶⁺ titration. The final $n_{\text{Fe}^{2+}}$ was recalculated by
281 normalising it to the initial volume of the solution (25 mL). We measured
282 significant amount of Fe²⁺ and determined a molar ratio $n_{\text{Fe}^{2+}}/n_{\text{S}^{2-}}$ of 1.7
283 (see Table B.2 in supplementary materials).

284 These two experiments clearly demonstrate that sample digestion in pres-
285 ence of S²⁻ reduces V⁵⁺ into V⁴⁺ and Fe³⁺ into Fe²⁺. These two redox reac-
286 tions artificially increase the FeO content, and therefore FeO/FeO_{total} ratio,
287 measured by colorimetry.

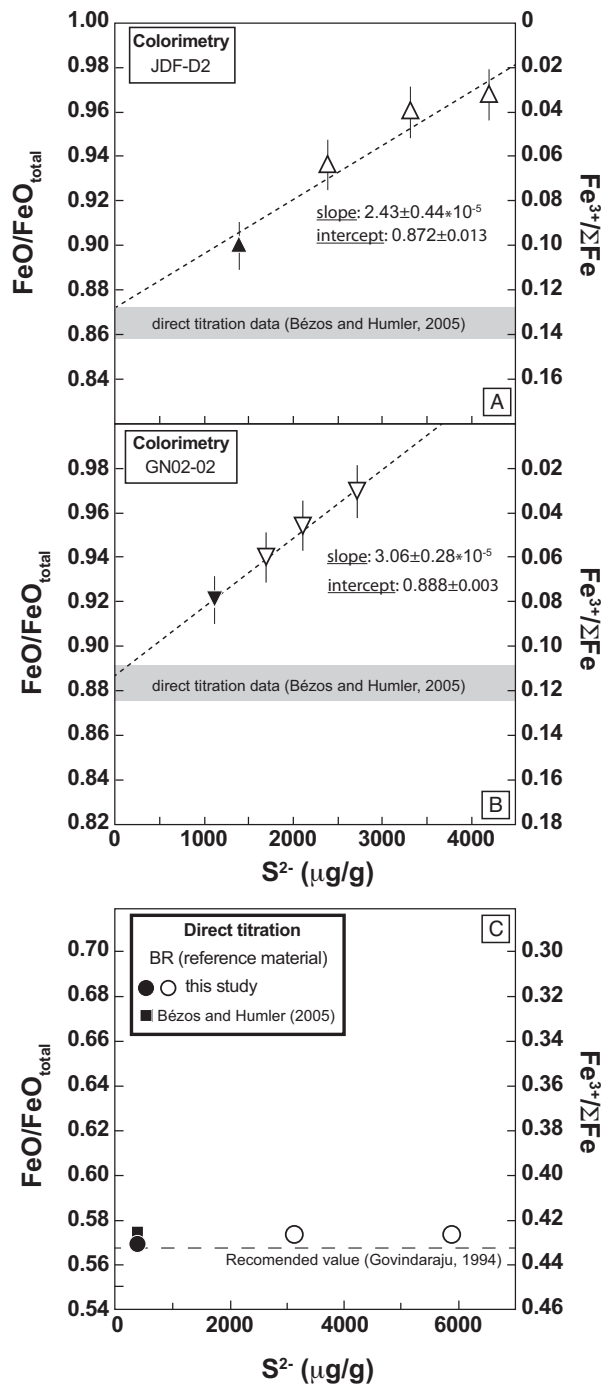


Figure 3: Quantification of sulfide (S^{2-}) interference on the FeO/FeO_{total} measurements for the vanadium-based colorimetric method (panels A and B) and for the direct titration method (panel C). A & B: experiments on the two natural MORB glassy matrices JDF-D2 and GN02-02, respectively. C: experiments on the BR basaltic rock reference material. Open symbols: samples spiked with varying amounts of a S^{2-} solution; solid symbols: un-spiked samples; Gray area: direct titration data from Bézoz and Humler (2005).

Our third experiment was designed to quantify the interference of S^{2-} on the measured FeO/FeO_{total} ratio in the presence of the sample matrix and under standard analytical conditions (section 3.1). Prior to sample dissolution, we added various amounts of S^{2-} to the natural glassy samples JDF-D2 and GN02-02. These two samples have natural sulfur contents of 1400 and 1128 $\mu g/g$ respectively (Bézoz, 2003), mostly in the form of S^{2-} . In Fig. 3, the solid symbols correspond to the results for un-spiked samples and open symbols to the S^{2-} -spiked samples. The higher the sulfide content is during sample digestion, the higher the measured FeO/FeO_{total} ratio. Because the slopes in Fig. 3 depend upon the $n_{Fe^{2+}}/n_{S^{2-}}$ mole ratio of the redox reaction and the total iron content, they cannot be compared directly. Therefore, we calculated from these data that for each mole of S^{2-} added to the JDF-D2 and GN-02-02 samples, 1.32 ± 0.24 and 1.29 ± 0.12 moles of Fe^{2+} were produced respectively. Although this mole ratio is slightly lower than those calculated from our two first experiments (i.e. 1.9-1.7), this result confirms that S^{2-} interferes under the standard analytical conditions of the colorimetric method. We also note that both mole ratios are close enough to suggest the same sulfide effect for both matrices.

308 *5.3.2. Direct titration method*

309 We first proceed to three dissolutions of the BR reference material — a
310 continental basalt, see Table A1 and A2 in appendix A — with no addition
311 of S^{2-} solution prior to sample digestion. The average ferrous iron content
312 recovered from these analyses is $6.59 \pm 0.04\%$ m/m (Table B.3), which is in
313 very good agreement with the recommended value of Govindaraju (1994) and
314 with the measurements from Bézos and Humler (2005) (6.57% and 6.65%,
315 respectively). Two dissolutions were then carried out in presence of varying
316 amount of a S^{2-} solution prepared from sodium sulfide hydrated salts (Na_2S).
317 The BR reference material contains naturally $390 \mu\text{g/g}$ of sulfur. Assuming
318 that this sulfur is in the -2 valence state, the sulfide concentrations of the
319 spiked experiments would thus be 3129 and 5870 $\mu\text{g/g}$ (Fig. 3 and Table B.3).
320 The measured ferrous iron contents of these two spiked-dissolutions yielded
321 6.63% for both experiments, which is indistinguishable from the sulfide-free
322 experiments ($6.59 \pm 0.04\%$ m/m) and from the recommended value (6.57
323 %, Govindaraju, 1994). These experiments suggest the absence of sulfide
324 interference in the case of the direct titration method.

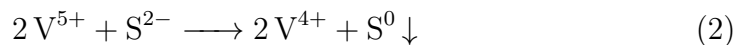
325 **6. Discussion**

326 Three important analytical results arise from our study. Firstly, our
327 vanadium-based colorimetric results for reference materials are in close agree-
328 ment with both the recommended values (Govindaraju, 1994; Jochum et al.,
329 2016) and the direct titration results from Bézos and Humler (2005). Sec-
330 ondly, the FeO and $\text{FeO}/\text{FeO}_{\text{total}}$ MORB data of Christie et al. (1986) can be
331 reproduced using the same sample powders and vanadium-based colorimet-

332 ric method (Fig. 2). Finally, our S^{2-} experiments demonstrate that reduced
333 sulfur clearly interferes with ferrous iron measurements in the case of the
334 vanadium-based wet chemistry whereas it has no effect during direct titra-
335 tion experiments. In the following discussion, we first review the nature of
336 the redox reactions triggered by the presence of S^{2-} during sample digestion.
337 We then discuss the implications of these results for the determination of the
338 iron redox state in MORB samples by wet chemistries. Finally, we compare
339 wet chemical results free of sulfide interaction to the most recent MORB data
340 obtained by XANES spectroscopy.

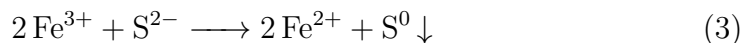
341 *6.1. Identifying the redox reactions with sulfide during the vanadium-based*
342 *wet chemistry*

343 The sulfide experiments designed in this study demonstrate that V^{5+} is
344 reduced to V^{4+} by the oxidation of S^{2-} . Sulfur exhibits mostly oxidation state
345 of -2, 0, +2, +4, and +6. According to the standard electrode potentials of
346 the vanadium, sulfur and iron redox couples of interest (see appendix C,
347 Fig. C.1), the spontaneous reaction that should occur involves the oxidant
348 having the strongest standard electrode potential and the reducing agent
349 of the couple having the lowest potential. Therefore, the predicted redox
350 reaction that prevails in our experiment is:



351 The reaction 2 will eventually stop when all the V^{5+} is reduced. However,
352 if the quantity of sulfides is large enough to ensure $n_{S^{2-}} > 0.5 \times n_{V^{4+}}$, then

353 the following redox reaction will take over:



354 Because pentavalent vanadium is added in large excess in the colorimetric
355 method, there is little chance that reaction 3 occurs during sample digestion.
356 Would this happen, the same effect would be expected on ferrous iron mea-
357 surements, as both equations have the same stoichiometric ratios of two. The
358 $n_{\text{V}^{4+}}$ or $n_{\text{Fe}^{2+}}$ to $n_{\text{S}^{2-}}$ mole ratios determined in our experiments, with, and
359 without sample matrix, are ≈ 1.8 and 1.3 , respectively. Although these re-
360 sults do not conform to the stoichiometric coefficients of reactions 2 and 3,
361 the identification of S^0 in our experiments — as black solid particles of mack-
362 inawite — indicates that the oxidation of sulfide may not proceed beyond
363 the formation of elemental sulfur. The low experimental mole ratios that
364 we determined from our experiments could result from several origins. First,
365 V^{5+} could react with other reduced vanadium species or with other reduced
366 polyvalent elements such as chromium. In terrestrial magmas, chromium
367 have a valence of +3 and vanadium, which partitions between the valences
368 of +3, +4 and +5, is largely dominated by the +4 valence (Sutton et al.,
369 2005; Papike, 2005). Once again, according to the standard redox potentials
370 of the half redox reactions reported in appendix C, none of these species
371 is expected to react spontaneously with V^{5+} . Such low mole ratios could
372 also be achieved if S^{2-} were to be lost during sample digestion in presence
373 of concentrated sulphuric acid — for example via the formation and partial
374 degassing of volatile compounds such as H_2S or SO_2 . We believe that the
375 lack of sulfide interference in the direct titration method could be explained

376 by such process which would be enhanced in boiling sulphuric acid (Zhang
377 et al., 2000). It may also be possible that the kinetic of eq. 3 is too slow com-
378 pared to the duration of the sample digestion (i.e. three minutes). Further
379 experimental work is clearly needed to understand how S^{2-} might escape or
380 be neutralized to different extent in both wet chemistries .

381 *6.2. Settling analytical discord between wet chemistries*

382 The study of Bézou and Humler (2005) was the first to suspect the pres-
383 ence of an analytical bias on the measurements of the iron redox state in
384 oceanic ridge basaltic glasses. The comparison of the vanadium-based colori-
385 metric data (Christie et al., 1986) with the direct (vanadium-free) titration
386 data (Bézou and Humler, 2005) revealed more reduced FeO/FeO_{total} ratios
387 when using the former analytical method. However, the lack of data on com-
388 mon reference materials between both studies hampered the clarification of
389 this analytical issue. Our study provides the keys to solve this analytical
390 discord.

391 First, we show that both wet chemistries agree for the reference mate-
392 rials FeO and FeO/FeO_{total} measurements (Fig. 1), but on the other hand
393 disagree when MORB samples are concerned (Fig. 2). There are important
394 differences between these two kinds of materials. The MORB samples display
395 glassy textures with high sulfur content ($S \approx 1000 \mu g/g$ Jenner and O'Neill,
396 2012), whereas the reference materials display fine-grained volcanic (BE-N,
397 BR, BHVO-1, BCR-1, JB-2) to coarse-grained plutonic (W-2) textures with
398 low sulfur contents ($S < 410 \mu g/g$, Table A.1). Second, our sulfide spiked
399 experiments clearly demonstrate that reduced sulfur interferes with ferrous
400 iron measurements in the case of the vanadium-based wet chemistry whereas

401 it does not for the direct titration method (section 6.1). Several studies
402 have analyzed the JDF-D2 sample — a MORB glass from the East Pacific
403 Rise from the study of Christie et al. (1986) — using either the vanadium-
404 based or the direct titration wet chemistries (Carmichael and Ghiorso, 1986;
405 Christie et al., 1986; Lange and Carmichael, 1989; Wallace and Carmichael,
406 1992; Nilsson and Peach, 1993; Bézoz and Humler, 2005). All data derived
407 from vanadium-based methods, whether they involved back-titration or col-
408 orimetric measurements (Carmichael and Ghiorso, 1986; Christie et al., 1986;
409 Lange and Carmichael, 1989; Wallace and Carmichael, 1992; Nilsson and
410 Peach, 1993, this study), present homogeneous but higher $\text{FeO}/\text{FeO}_{\text{total}}$ ra-
411 tios (>0.910) compared to the direct titration data (0.864 ± 0.007 , Bézoz and
412 Humler, 2005). This confirms that the S^{2-} derived from the sample ma-
413 trix contributes, just as the S^{2-} added to the experiments, to increase the
414 $\text{FeO}/\text{FeO}_{\text{total}}$ ratio during sample digestion. A classical counter-argument
415 would be to explain such difference by the undesired oxidation of Fe^{2+} to
416 Fe^{3+} by atmospheric O_2 in the case of the direct titration method. It is
417 for this specific reason that Wilson (1960) developed the vanadium-based
418 method. However, this issue has been examined in details by Bézoz and
419 Humler (2005) as notified in the introduction (see section 1).

420 On the basis on the sulfide-bearing experiments carried out on the JDF-
421 D2 and GN02-02 MORB glassy samples, we propose to define a colorimetric
422 sulfide-free $\text{FeO}/\text{FeO}_{\text{total}}$ ratio which might be retrieved from the intercept
423 values of the linear regressions in Fig. 3. The resulting sulfide-free ratios
424 agree within error with the direct titration data of Bézoz and Humler (2005)
425 (Table 1 and Fig. 3). This approach demonstrates that ferrous iron deter-

426 mination by different wet chemistries on MORB samples can be reconciled
 427 if vanadium-based data are corrected for sulfide interference.

	FeO		FeO _{total}		FeO/FeO _{total}
	Method	Wt.%	Method	Wt.%	
JDF-D2					
Carmichael and Ghiorso (1986)	Colorimetry ⁽¹⁾	11.11		12.14 ⁽³⁾	0.915
Christie et al. (1986)	Colorimetry ⁽¹⁾	11.08			
	Back-titration ⁽¹⁾	11.11			
Nilsson and Peach (1993)	Colorimetry ⁽¹⁾	11.07	EMPA	12.17	0.910
Lange and Carmichael(1989)	Colorimetry ⁽¹⁾	10.93			
	Back-titration ⁽¹⁾	11.12			
Wallace and Carmichael (1992)	Colorimetry ⁽¹⁾	11.08	EMPA	12.09	0.916
Bézos and Humler (2005)	Direct titration	10.52 ± 0.05	EMPA	12.17 ± 0.08	0.864 ± 0.007
This study	Colorimetry ⁽¹⁾	10.99 ± 0.05	Colorimetry	11.99 ± 0.09	0.917 ± 0.011
	Sulfide-free ratio ⁽²⁾				0.872 ± 0.013
Cottrell and Kelley (2010)	XANES spectroscopy				0.833 ± 0.004
Zhang et al. (2018)	XANES spectroscopy				0.849 ± 0.010
Berry et al. (2018)	XANES spectroscopy				0.876 ± 0.010
GN02-02					
Bézos and Humler (2005)	Direct titration	8.50 ± 0.04	EMPA	9.61 ± 0.07	0.884 ± 0.008
This study	Colorimetry ⁽¹⁾	8.72 ± 0.06	Colorimetry	9.49 ± 0.11	0.918 ± 0.011
	Sulfide-free ratio ⁽²⁾				0.888 ± 0.003

Table 1: Compilation of JDF-D2 and GN02-02 measurements by wet chemistries and XANES spectroscopic methods. ⁽¹⁾: Vanadium-based wet chemical methods; ⁽²⁾ ratio corrected for sulfide interference; ⁽³⁾ LDEO (Lamont -Doherty Earth Laboratory) reference value (Christie et al., 1986); EMPA: Electron Micro-Probe Analyzer.

428 6.3. The FeO/FeO_{total} ratio of MORB glasses

429 The average FeO/FeO_{total} ratio of the 49 MORB glasses analyzed in
 430 this study by the colorimetric method is 0.92±0.01 (Fig. 4a). This result
 431 agrees with the average ratio of 0.93±0.02 from Christie et al. (1986) (Fig.
 432 4b). Christie et al. (1986) data can therefore be reproduced not only for
 433 the JDF D2 sample but also for a sample set representative of the global
 434 MORB database of Bézos and Humler (2005). As we have demonstrated

435 that vanadium-based wet chemistries overestimate the $\text{FeO}/\text{FeO}_{\text{total}}$ ratio,
436 the average MORB ratio that we report in this study should be corrected
437 for sulfide interference. This could be done for example by using the sulfur
438 content of each sample — assuming 100% S^{2-} (Mathez, 1976; Métrich et al.,
439 2009) — and by applying the $n_{\text{Fe}^{2+}}/n_{\text{S}^{2-}}$ reaction ratio of ≈ 1.30 (see section
440 5.3) to calculate the sulfide-free ratios. When using the sulfur data deter-
441 mined by Bézos (2003) and Bézos et al. (2005) on the MORB analyzed in
442 this study, such first order correction gives a $\text{FeO}/\text{FeO}_{\text{total}}$ ratio of 0.89 ± 0.02
443 (Fig. 4a). However, in the absence of more comprehensive data exploring
444 the behaviour of the $n_{\text{Fe}^{2+}}/n_{\text{S}^{2-}}$ ratio during analysis of MORB matrices, we
445 do not recommend to use the vanadium-based wet chemistry to analyze the
446 ferrous iron content of S^{2-} -bearing samples.

447 Although we have demonstrated that ferrous iron data from Bézos and
448 Humler (2005) are not affected by the presence of sulfide, we must put a
449 caveat with respect to their calculated $\text{FeO}/\text{FeO}_{\text{total}}$ ratio that is not strictly
450 speaking self-consistent (Cottrell and Kelley, 2011; Berry et al., 2018). In-
451 deed, this latter study measured the $\text{FeO}_{\text{total}}$ in MORB glasses using an
452 Electron Micro-Probe Analyzer (EMPA) whereas the ferrous iron were de-
453 termined on sample powders by direct titration. Bulk analyses were thus
454 normalised to in-situ data. Even if both analytical methods are highly reli-
455 able, they do not refer to the exact same material. Indeed, as mentioned in
456 section 5.2, the glass powders prepared for ferrous iron analysis may contain
457 variable amount of plagioclase micro-crystals from sample to sample. As a
458 consequence, in Fig. 2 the bulk colorimetric $\text{FeO}_{\text{total}}$ data display systemati-
459 cally lower contents compared to the in-situ EMPA data gather by Bézos and

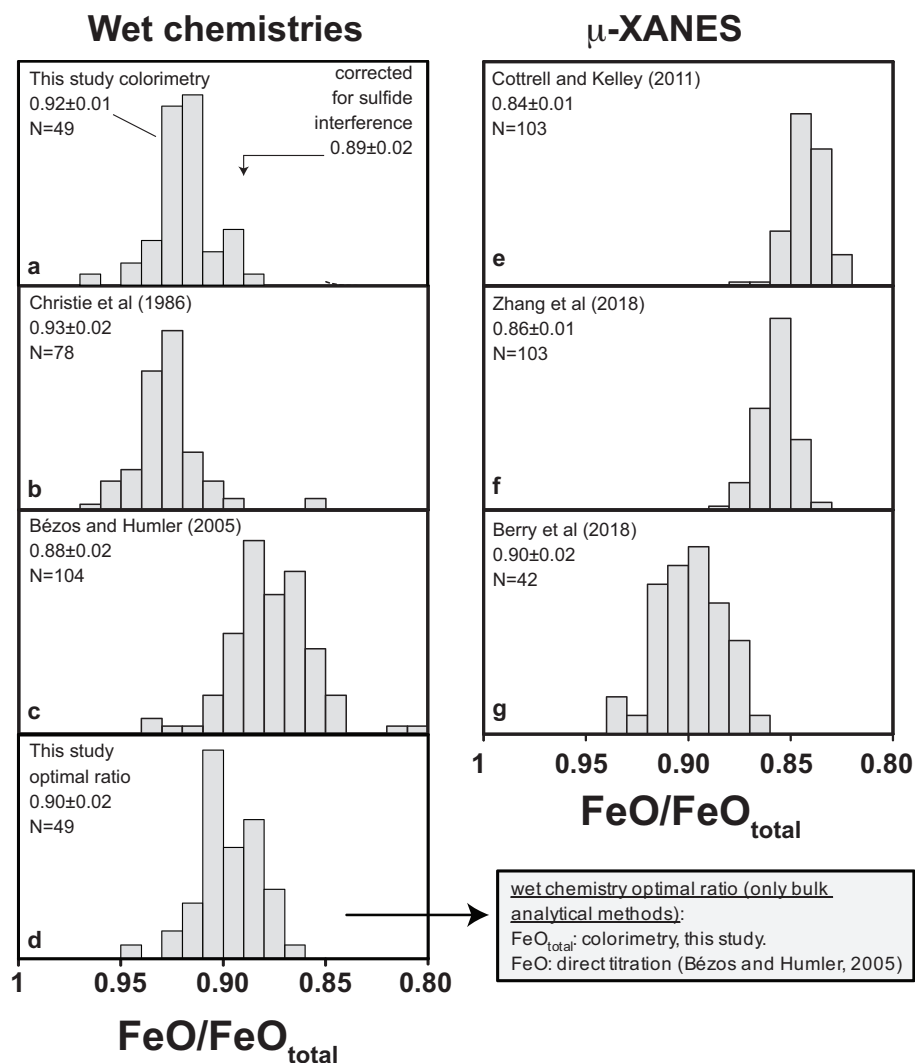


Figure 4: Comparison of the $\text{FeO}/\text{FeO}_{\text{total}}$ histograms (bin size 0.01, origin 1) of MORB glasses determined by wet chemistry: (a) colorimetry, this study; (b) colorimetry, Christie et al. (1986); (c) direct titration, Bézoz and Humler (2005); (d) optimal wet chemistry ratio (FeO (Bézoz and Humler (2005))/ $\text{FeO}^{\text{total}}$ (this study) and by μ -XANES: (e) Cottrell and Kelley (2011); (f) Zhang et al. (2018); (g) Berry et al. (2018). N: number of sample analyzed. The standard deviation of the average ratio is reported in each panel. Arrow in panel (a): average ratio of colorimetric data corrected for sulfide interference (see section 6.3).

460 Humler (2005) on the corresponding chips of glass. Such difference could be
461 accounted for by the presence of ≈ 1.5 weight % plagioclase micro-crystals
462 in MORB glassy rims (Bézos and Humler, 2005). As mentioned by Bézos
463 and Humler (2005), if their ferrous iron analysis were to be corrected for the
464 presence of such micro-crystals in sample powders, the ratio would increased
465 from 0.88 ± 0.02 to 0.89 ± 0.02 . However, such first order correction should not
466 be applied to single analyses. Some samples might have negligible amounts
467 of micro-crystals as it is, for example, the case for the JDF-D2 and GN02-02
468 samples that display both similar bulk and in-situ $\text{FeO}_{\text{total}}$ contents (Table
469 1).

470 On the other hand, the presence of olivine micro-crystals ($\text{FeO} > 15$ %m/m)
471 in the sample powders would inevitably distort wet chemical results (Cot-
472 trell and Kelley, 2011). However, given the plagioclase-to-olivine abundance
473 ratio of $\sim 70:30$ — expected from the cotectic crystallisations of MORB
474 (Grove et al., 1992), and the relatively low plagioclase contents in our sam-
475 ple powders ($< 1.5\%$ on average), the presence of such small amounts of
476 olivine in our sample powders would have no noticeable effect on the mea-
477 sured $\text{FeO}/\text{FeO}_{\text{total}}$ ratio, as long as $\text{FeO}_{\text{total}}$ is measured on the same sample
478 powders as FeO .

479 We calculated a self consistent $\text{FeO}/\text{FeO}_{\text{total}}$ ratio — that we named the
480 optimal ratio — of 0.90 ± 0.02 (Fig. 4d) using the bulk FeO and $\text{FeO}_{\text{total}}$
481 data from Bézos and Humler (2005) and this study, respectively. This result
482 agrees within uncertainty with the plagioclase corrected ratio (0.89 ± 0.02) of
483 Bézos and Humler (2005) and with the colorimetric sulfide-free ratio from
484 this study (0.89 ± 0.02 , Fig. 4a).

485 *6.4. Comparison of wet chemical and XANES spectroscopic data*

486 The iron redox state of the JDF-D2 sample has not only been deter-
487 mined many times by wet chemistry (section 6.2), but also by XANES spec-
488 troscopy (see Table 1: Cottrell and Kelley, 2011; Zhang et al., 2018; Berry
489 et al., 2018). One critical aspect of this spectroscopic method resides in the
490 calibration of XANES spectra using an independent technique. To date, the
491 Mössbauer spectroscopy has been the most widely used method to determine
492 the $\text{FeO}/\text{FeO}_{\text{total}}$ ratio of calibration materials (Cottrell et al., 2009; Zhang
493 et al., 2018; Berry et al., 2018; Farges et al., 2004). However, the acquisi-
494 tion and interpretation of Mössbauer analyses is a matter of active debate in
495 the literature (Cottrell et al., 2009; Zhang et al., 2018; Berry et al., 2018).
496 The detailed discussion on the difference of Mössbauer data used to cali-
497 brate XANES data is beyond the scope of this paper, but it involves, among
498 other things, varying temperature of data acquisition and the interpretation
499 of the most reduced spectra (Cottrell et al., 2009; Zhang et al., 2018; Berry
500 et al., 2018). As an illustration of this analytical difficulty, the XANES
501 $\text{FeO}/\text{FeO}_{\text{total}}$ ratios measured on the JDF-D2 sample vary from 0.833 up to
502 0.876 (Table 1). Even when considering the improved Mössbauer calibration
503 of Zhang et al. (2018), the XANES JDF-D2 data appeared to be more varied
504 than wet chemical data free of sulfide interference (Bézos and Humler (2005)
505 and sulfide-free ratio from this study, see Table 4). Notably, these latter
506 chemical data agree within errors with the XANES JDF-D2 data from Berry
507 et al. (2018) (Table 1).

508 The comparison of the global MORB data base reveals the same differ-
509 ences as those observed on the JDF-D2 (Fig. 4). The study of Cottrell et al.

510 (2009) reports the lowest average $\text{FeO}/\text{FeO}_{\text{total}}$ ratio of 0.84 ± 0.01 (Fig.4e),
511 the study of Zhang et al. (2018) re-evaluates this ratio to be 0.86 ± 0.01
512 (Fig.4f), and finally, the study of Berry et al. (2018) reports the most re-
513 duced XANES data with an average value of 0.90 ± 0.02 (Fig. 4g). In line
514 with the JDF-D2 results, the XANES results of Berry et al. (2018) agree
515 within uncertainty with sulfide-free, plagioclase-corrected or optimal ratios
516 determined in this study (Table 1 and Fig. 4).

517 7. Conclusions

518 New colorimetric measurements of the iron redox state ratio for the se-
519 lected reference materials and MORB glasses from the study of Bézos and
520 Humler (2005) and Christie et al. (1986) revealed the presence of an analyti-
521 cal bias between the colorimetric and the direct titration methods. Both wet
522 chemistries agree on reference materials but not on MORB samples. The
523 colorimetric measurements display on MORB samples systematically more
524 reduced $\text{FeO}/\text{FeO}_{\text{total}}$ ratios (0.93-0.92: Christie et al., 1986, this study) com-
525 pared to direct titration data (Bézos and Humler, 2005, 0.88:).

526 We have established that the presence of reduced sulfur in MORB sam-
527 ples interferes with ferrous iron measurements in the case of the colorimetric
528 method whereas it has no effect on direct titration measurements. This dif-
529 ference of behaviour is certainly related to the difference of sample digestion
530 procedures between both methods. We demonstrated on two MORB sam-
531 ples that, when corrected for the interference of S^{2-} , colorimetric data agree
532 within uncertainty with direct titration data.

533 The average $\text{FeO}/\text{FeO}_{\text{total}}$ ratio of 49 MORB glasses calculated from the

534 bulk FeO and FeO_{total} data from Bézou and Humler (2005) and this study,
535 respectively, is 0.90 ± 0.02 . Acknowledging that MORB colorimetric data
536 need to be corrected for the interference of sulfide and that the FeO/FeO_{total}
537 ratio of Bézou and Humler (2005) needs to be corrected for the presence
538 of plagioclase micro-crystals in the sample powders, all the wet chemical
539 methods agree within errors. This result is also consistent with the XANES
540 data from Berry et al. (2018).

541 **Acknowledgments**

542 We would like to thanks M. Rivoal and E. Le Menn for their analytical
543 assistance with the spectrophotometer and Raman spectrometer. Comments
544 by M. Brounce, A. Berry, and an anonymous reviewer greatly helped to
545 improve the manuscript. We also thank Viviane Guilly for assistance with
546 the english text. This work was supported by the program TelluS-SYSTER
547 (Système Terre: processus et couplage) of CNRS/INSU.

548 **References**

- 549 Berry, A.J., Stewart, G.A., O'Neill, H.S., Mallmann, G., Mosselmans,
550 J.F.W., 2018. A re-assessment of the oxidation state of iron in morb
551 glasses. *Earth and Planetary Science Letters* 483, 114 – 123. doi:<https://doi.org/10.1016/j.epsl.2017.11.032>.
552
- 553 Bézou, A., 2003. Etude des elements lithophiles et fortement siderophiles
554 (Pd, Pt, Ru et Ir) dans les basaltes des dorsales oceaniques. Ph.D. thesis.
555 Universite de Paris 7 Denis Diderot, France.

- 556 Bézou, A., Humler, E., 2005. The $Fe^{3+}/\Sigma Fe$ ratios of MORB glasses and
557 their implications for mantle melting. *Geochimica et Cosmochimica Acta*
558 69, 711–725. doi:10.1016/j.gca.2004.07.026.
- 559 Bézou, A., Lorand, J.P., Humler, E., Gros, M., 2005. Platinum-group ele-
560 ment systematics in Mid-Oceanic Ridge basaltic glasses from the Pacific,
561 Atlantic, and Indian Oceans. *Geochimica et Cosmochimica Acta* 69, 2613–
562 2627. doi:10.1016/j.gca.2004.10.023.
- 563 Bourdoiseau, J.A., Jeannin, M., Sabot, R., Rmazeilles, C., Refait, P., 2008.
564 Characterisation of mackinawite by raman spectroscopy: Effects of crys-
565 tallisation, drying and oxidation. *Corrosion Science* 50, 3247 – 3255.
566 doi:https://doi.org/10.1016/j.corsci.2008.08.041.
- 567 Brounce, M., Kelley, K.A., Cottrell, E., Reagan, M.K., 2015. Temporal
568 evolution of mantle wedge oxygen fugacity during subduction initiation.
569 *Geology* 43, 775–778. doi:10.1130/G36742.1.
- 570 Brounce, M., Stolper, E., Eiler, J., 2017. Redox variations in Mauna Kea
571 lavas, the oxygen fugacity of the Hawaiian plume, and the role of volcanic
572 gases in Earth’s oxygenation. *Proceedings of the National Academy of*
573 *Science* 114, 8997–9002. doi:10.1073/pnas.1619527114.
- 574 Carmichael, I.S.E., Ghiorso, M.S., 1986. Oxidation-reduction relations in
575 basic magma: a case for homogeneous equilibria. *Earth and Planetary*
576 *Science Letters* 78, 200–210. doi:10.1016/0012-821X(86)90061-0.
- 577 Chin, E.J., Shimizu, K., Bybee, G.M., Erdman, M.E., 2018. On the devel-
578 opment of the calc-alkaline and tholeiitic magma series: A deep crustal

- 579 cumulate perspective. *Earth and Planetary Science Letters* 482, 277–287.
580 doi:10.1016/j.epsl.2017.11.016.
- 581 Christie, D.M., Carmichael, I.S.E., Langmuir, C.H., 1986. Oxidation states
582 of mid-ocean ridge basalt glasses. *Earth and Planetary Science Letters* 79,
583 397–411. doi:10.1016/0012-821X(86)90195-0.
- 584 Cottrell, E., Kelley, K.A., 2011. The oxidation state of Fe in MORB glasses
585 and the oxygen fugacity of the upper mantle. *Earth and Planetary Science*
586 *Letters* 305, 270–282. doi:10.1016/j.epsl.2011.03.014.
- 587 Cottrell, E., Kelley, K.A., Lanzirotti, A., Fischer, R.A., 2009. High-precision
588 determination of iron oxidation state in silicate glasses using XANES.
589 *Chemical Geology* 268, 167–179.
- 590 Crabtree, S.M., Lange, R.A., 2012. An evaluation of the effect of degassing on
591 the oxidation state of hydrous andesite and dacite magmas: a comparison
592 of pre- and post-eruptive Fe²⁺ concentrations. *Contributions to Mineralogy*
593 *and Petrology* 163, 209–224. doi:10.1007/s00410-011-0667-7.
- 594 Farges, F., Lefrère, Y., Rossano, S., Berthereau, A., Calas, G., Brown, Jr.,
595 G.E., 2004. The effect of redox state on the local structural environment
596 of iron in silicate glasses: a combined XAFS spectroscopy, molecular dy-
597 namics, and bond valence study. *Journal of Non Crystalline Solids* 344,
598 176–188. doi:10.1016/j.jnoncrysol.2004.07.050.
- 599 Fialin, M., Bézou, A., Wagner, C., Magnien, V., Humler, E., 2004. Quan-
600 titative electron microprobe analysis of Fe³⁺/∑Fe: Basic concepts and

- 601 experimental protocol for glasses. *American Mineralogist* 89, 654–662.
602 doi:10.2138/am-2004-0421.
- 603 Gaborieau, M., Laubier, M., Bolfan-Casanova, N., McCammon, C., Van-
604 telon, D., Chumakov, A., Schiavi, F., Neuville, D., Venugopal, S., 2020. De-
605 termination of $\text{Fe}^{3+}/\Sigma\text{Fe}$ of olivine-hosted melt inclusions using mössbauer
606 and xanes spectroscopy. *Chemical Geology* 547, 119646. doi:<https://doi.org/10.1016/j.chemgeo.2020.119646>.
607 //doi.org/10.1016/j.chemgeo.2020.119646.
- 608 Gill, J.B., 1981. *Orogenic andesites and plate tectonics* / James B. Gill.
609 Springer-Verlag Berlin ; New York.
- 610 Govindaraju, K., 1994. 1994 compilation of working values and sample
611 description for 383 geostandards. *Geostandards Newsletter* 18, 1–158.
612 doi:10.1046/j.1365-2494.1998.53202081.x-i1.
- 613 Grillot, H., Boucetta, M., Rouquette, C., A., S., 1964. Methode d'analyse
614 quantitative appliques roches et aux prlvements de la prospection gochim-
615 ique. BRGM. pp. 1–3319.
- 616 Grocke, S.B., Cottrell, E., de Silva, S., Kelley, K.A., 2016. The role of
617 crustal and eruptive processes versus source variations in controlling the
618 oxidation state of iron in Central Andean magmas. *Earth and Planetary
619 Science Letters* 440, 92–104. doi:10.1016/j.epsl.2016.01.026.
- 620 Grove, T.L., Kinzler, R.J., Bryan, W.B., 1992. Fractionation of mid-ocean
621 ridge basalt (MORB). Washington DC American Geophysical Union Geo-
622 physical Monograph Series 71, 281–310. doi:10.1029/GM071p0281.

- 623 Hartley, M.E., Shorttle, O., Maclennan, J., Moussallam, Y., Edmonds, M.,
624 2017. Olivine-hosted melt inclusions as an archive of redox heterogeneity
625 in magmatic systems. *Earth and Planetary Science Letters* 479, 192–205.
626 doi:10.1016/j.epsl.2017.09.029.
- 627 Holland, H.D., 2002. Volcanic gases, black smokers, and the great oxidation
628 event. *Geochimica et Cosmochimica Acta* 66, 3811–3826. doi:10.1016/
629 S0016-7037(02)00950-X.
- 630 Jenner, F.E., O'Neill, H.S.C., 2012. Analysis of 60 elements in 616 ocean
631 floor basaltic glasses. *Geochemistry, Geophysics, Geosystems* 13, Q02005.
632 doi:10.1029/2011GC004009.
- 633 Jochum, K.P., Weis, U., Schwager, B., Stoll, B., Wilson, S.A., Haug, G.H.,
634 Andreae, M.O., Enzweiler, J., 2016. Reference values following iso guide-
635 lines for frequently requested rock reference materials. *Geostandards and*
636 *Geoanalytical Research* 40, 333–350. doi:10.1111/j.1751-908X.2015.
637 00392.x.
- 638 Kelley, K.A., Cottrell, E., 2012. The influence of magmatic differentiation
639 on the oxidation state of Fe in a basaltic arc magma. *Earth and Planetary*
640 *Science Letters* 329, 109–121. doi:10.1016/j.epsl.2012.02.010.
- 641 Kress, V.C., Carmichael, I.S.E., 1991. The compressibility of silicate liquids
642 containing Fe₂O₃ and the effect of composition, temperature, oxygen fu-
643 gacity and pressure on their redox states. *Contributions to Mineralogy and*
644 *Petrology* 108, 82–92. doi:10.1007/BF00307328.

- 645 Lange, R.A., Carmichael, I.S.E., 1989. Ferric-ferrous equilibria in Na₂O-FeO-
646 Fe₂O₃-SiO₂ melts: Effects of analytical techniques on derived partial molar
647 volumes. *Geochimica and Cosmochimica Acta* 53, 2195–2204. doi:10.
648 1016/0016-7037(89)90343-8.
- 649 Le Losq, C., Berry, A.J., Kendrick, M.A., Neuville, D.R., O'Neill, H.S.C.,
650 2019. Determination of the oxidation state of iron in Mid-Ocean Ridge
651 basalt glasses by Raman spectroscopy. *American Mineralogist* 104, 1032–
652 1042. doi:10.2138/am-2019-6887.
- 653 Mathez, E.A., 1976. Sulfur solubility and magmatic sulfides in submarine
654 basalt glass. *Journal of Geophysical Research* 81, 4269–4276. doi:10.
655 1029/JB081i023p04269.
- 656 Métrich, N., Berry, A.J., O'Neill, H.S.C., Susini, J., 2009. The oxidation state
657 of sulfur in synthetic and natural glasses determined by X-ray absorption
658 spectroscopy. *Geochimica and Cosmochimica Acta* 73, 2382–2399. doi:10.
659 1016/j.gca.2009.01.025.
- 660 Mysen, B.O., Carmichael, I.S.E., Virgo, D., 1985. A comparison of iron redox
661 ratios in silicate glasses determined by wet-chemical and ⁵⁷Fe Mossbauer
662 resonant absorption methods. *Contribution to Mineralogy and Petrology*
663 90, 101–106.
- 664 Nilsson, K., Peach, C.L., 1993. Sulfur speciation, oxidation state, and sulfur
665 concentration in backarc magmas. *Geochimica Cosmochimica Acta* 57,
666 3807–3813. doi:10.1016/0016-7037(93)90158-S.

- 667 Novella, D., Maclennan, J., Shorttle, O., Prytulak, J., Murton, B.J., 2020. A
668 multi-proxy investigation of mantle oxygen fugacity along the Reykjanes
669 Ridge. *Earth and Planetary Science Letters* 531, 115973. doi:10.1016/j.
670 *epsl*.2019.115973.
- 671 O'Neill, H.S.C., Berry, A.J., Mallmann, G., 2018. The oxidation state of
672 iron in Mid-Ocean Ridge Basaltic (MORB) glasses: Implications for their
673 petrogenesis and oxygen fugacities. *Earth and Planetary Science Letters*
674 504, 152–162. doi:10.1016/j.*epsl*.2018.10.002.
- 675 Papike, J.J., 2005. Comparative planetary mineralogy: Valence state parti-
676 tioning of Cr, Fe, Ti, and V among crystallographic sites in olivine, pyrox-
677 ene, and spinel from planetary basalts. *American Mineralogist* 90, 277–290.
678 doi:10.2138/am.2005.1779.
- 679 Roex, A.P.L., Watkins, R.T., 1995. A rapid ion chromatographic method
680 for the determination of the $\text{Fe}^{3+}/\text{Fe}^{2+}$ ratio in silicate rocks and minerals.
681 *Geochemical Journal* 29, 85–89. doi:10.2343/*geochemj*.29.85.
- 682 Rossano, S., Balan, E., Morin, G., Bauer, J.P., Calas, G., Brouder, C., 1999.
683 ^{57}Fe Mössbauer spectroscopy of tektites. *Physics and Chemistry of Min-
684 erals* 26, 530–538. doi:10.1007/s002690050216.
- 685 Saikkonen, R.J., Rautiainen, L.A., 1993. Determination of ferrous iron in
686 rock and mineral samples by three volumetric methods. *Bulletin of Geo-
687 logical Society of Finland* 65.
- 688 Schuessler, J.A., Botcharnikov, R.E., Behrens, H., Misiti, V., Freda, C., 2008.
689 *Amorphous Materials: Properties, structure, and Durability: Oxidation*

- 690 state of iron in hydrous phono-tephritic melts. *American Mineralogist* 93,
691 1493–1504. doi:10.2138/am.2008.2795.
- 692 Shorttle, O., Moussallam, Y., Hartley, M.E., MacLennan, J., Edmonds, M.,
693 Murton, B.J., 2015. Fe-XANES analyses of Reykjanes Ridge basalts: Im-
694 plications for oceanic crust's role in the solid Earth oxygen cycle. *Earth*
695 *and Planetary Science Letters* 427, 272–285. doi:10.1016/j.eps1.2015.
696 07.017.
- 697 Sinton, J.M., 2003. Magma Genesis and Mantle Heterogeneity in the Manus
698 Back-Arc Basin, Papua New Guinea. *Journal of Petrology* 44, 159–195.
699 doi:10.1093/petrology/44.1.159.
- 700 Sossi, P.A., O'Neill, H.S.S., 2011. Systematic underestimation of the oxida-
701 tion state of MORB glasses. *Mineral. Mag.* 75, 1915.
- 702 Sutton, S.R., Karner, J., Papike, J., Delaney, J.S., Shearer, C., Newville,
703 M., Eng, P., Rivers, M., Dyar, M.D., 2005. Vanadium K edge XANES of
704 synthetic and natural basaltic glasses and application to microscale oxygen
705 barometry. *Geochimica Cosmochimica Acta* 69, 2333–2348. doi:10.1016/
706 j.gca.2004.10.013.
- 707 Tarafder, P.K., Thakur, R., 2013. An optimised 1,10-phenanthroline method
708 for the determination of ferrous and ferric oxides in silicate rocks, soils and
709 minerals. *Geostandards and Geoanalytical Research* 37, 155–168. doi:10.
710 1111/j.1751-908X.2012.00183.x.
- 711 Wallace, P., Carmichael, I.S.E., 1992. Sulfur in basaltic magmas. *Geochimica*
712 *Cosmochimica Acta* 56, 1863–1874. doi:10.1016/0016-7037(92)90316-B.

- 713 Wilson, A.D., 1960. The micro-determination of ferrous iron in silicate min-
714 erals by a volumetric and a colorimetric method. *The Analyst* 85, 823.
715 doi:10.1039/an9608500823.
- 716 Yokoyama, T., Nakamura, E., 2002. Precise determination of
717 ferrous iron in silicate rocks. *Geochimica et Cosmochimica*
718 *Acta* 66, 1085 – 1093. URL: [http://www.sciencedirect.com/
719 science/article/pii/S0016703701008092](http://www.sciencedirect.com/science/article/pii/S0016703701008092), doi:[https://doi.org/10.
720 1016/S0016-7037\(01\)00809-2](https://doi.org/10.1016/S0016-7037(01)00809-2).
- 721 Zhang, H.L., Cottrell, E., Solheid, P.A., Kelley, K.A., Hirschmann, M.M.,
722 2018. Determination of $\text{Fe}^{3+}/\Sigma\text{Fe}$ of XANES basaltic glass standards by
723 Mössbauer spectroscopy and its application to the oxidation state of iron in
724 MORB. *Chemical Geology* 479, 166–175. doi:10.1016/j.chemgeo.2018.
725 01.006.
- 726 Zhang, Q., Dalla Lana, I.G., Chuang, K.T., Wang, H., 2000. Reactions be-
727 tween hydrogen sulfide and sulfuric acid: a novel process for sulfur removal
728 and recovery. *Industrial & Engineering Chemistry Research* 39, 2505–2509.
729 doi:10.1021/ie990717z.